

FIRST EXPERIMENTAL OBSERVATIONS OF THE PLASMA-CASCADE INSTABILITY IN THE CeC PoP ACCELERATOR

Irina Petrushina, Yichao Jing, Jun Ma, Igor Pinayev, Gang Wang, Kai Shih, Yuan Hui Wu, Vladimir N. Litvinenko

TUPLM07

Brookhaven National Laboratory, Upton, Long Island, New York, USA
Stony Brook University, Stony Brook, Long Island, New York, USA

Abstract

Preservation of the beam quality is important for attaining the desirable properties of the beam. Collective effects can produce an instability severely degrading beam emittance, momentum spread and creating filamentation of the beam. Microbunching instability for beams traveling along a curved trajectory, and space charge driven parametric transverse instabilities are well-known and in-depth studied. However, none of the above include a microbunching longitudinal instability driven by modulations of the transverse beam size. This phenomenon was observed for the first time during the commissioning of the CeC PoP experiment. Based on the dynamics of this instability we named it a Plasma-Cascade Instability (PCI). PCI can strongly intensify longitudinal micro-bunching originating from the beam's shot noise, and even saturate it. Resulting random density and energy microstructures in the beam can become a serious problem for generating high quality electron beams. On the other hand, such instability can drive novel high-power sources of broadband radiation. In this paper we present our experimental observations of the PCI and the supporting results of the numerical simulations.



Fig. 1: Panoramic view of the CeC system installed in IP2.

Coherent electron Cooling Proof of Principle Experiment

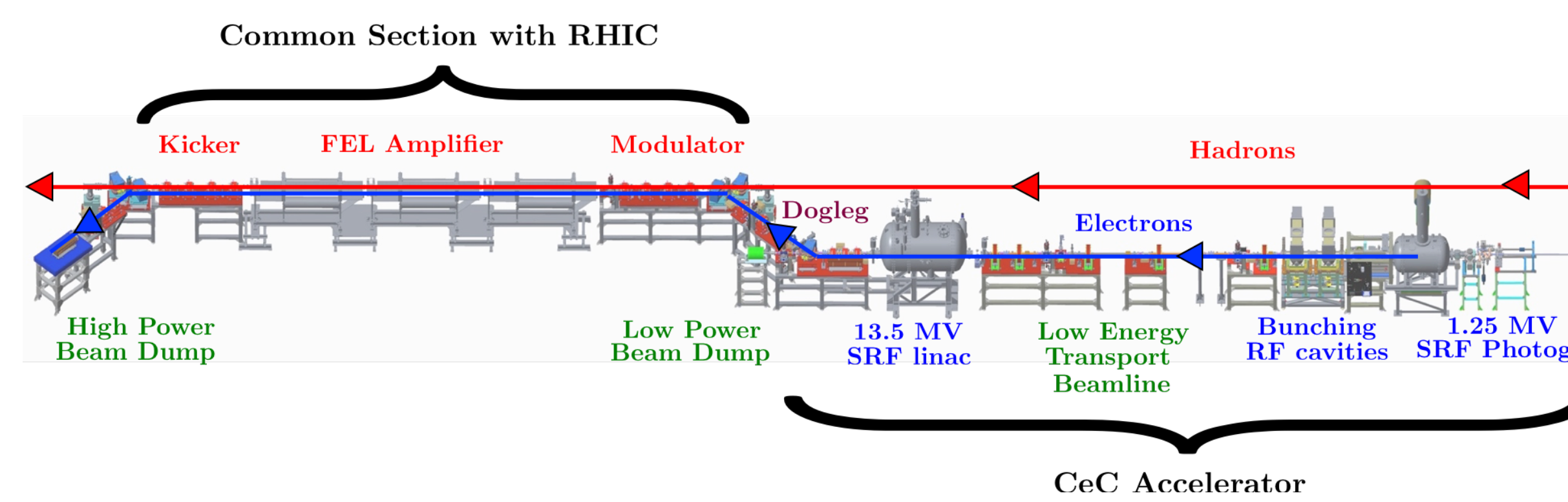


Fig. 2: Layout of the CeC system and its accelerator

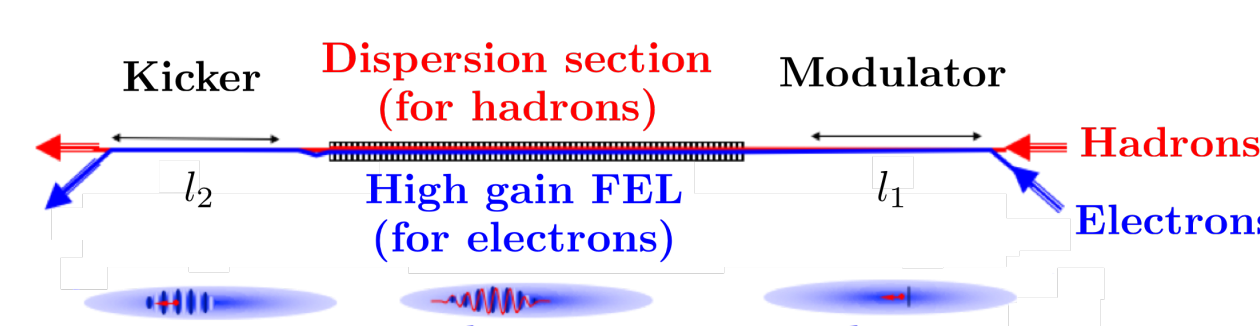


Fig. 3: Economic version of CeC, where electron and hadron beams are not separated.

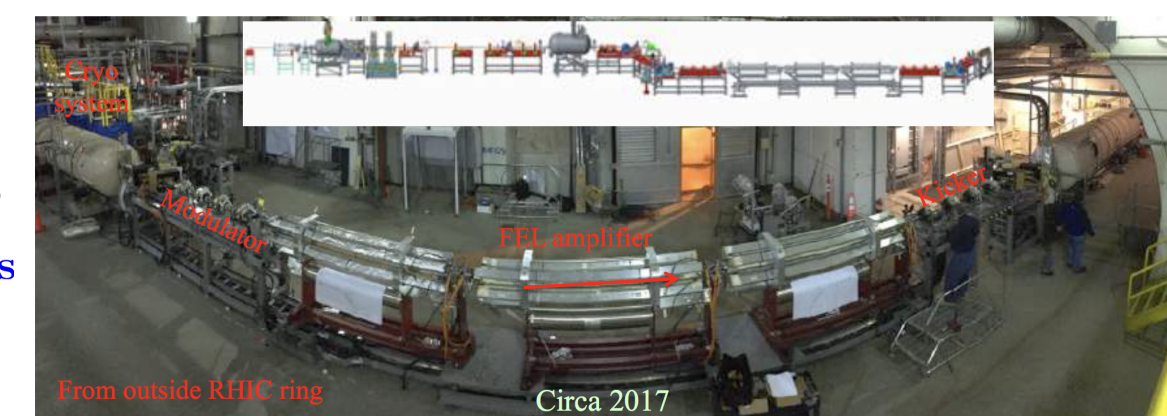


Fig. 4: Panoramic view of the CeC system installed in IP2.

Parameter	Design	Status	Comment
Species in RHIC (GeV/u)	Au ⁺⁷⁹ 40	Au ⁺⁷⁹ 26.5	to match e-beam
Electron energy (MeV)	21.95	14.56	linac quench
Charge per electron bunch (nC)	0.5-5	0.1-10.7	✓
Peak current (A)	100	50-100	✓
Bunch duration (psec)	10-50	12	✓
Normalized beam emittance (mm-mrad)	< 5	3-5	✓
Energy spread, RMS (%)	0.1	0.1	✓
FEL wavelength (μm)	13	31	new IR diagnostics
Repetition rate (kHz)	78.18	78.18	✓
CW beam (μA)	< 400	150	✓

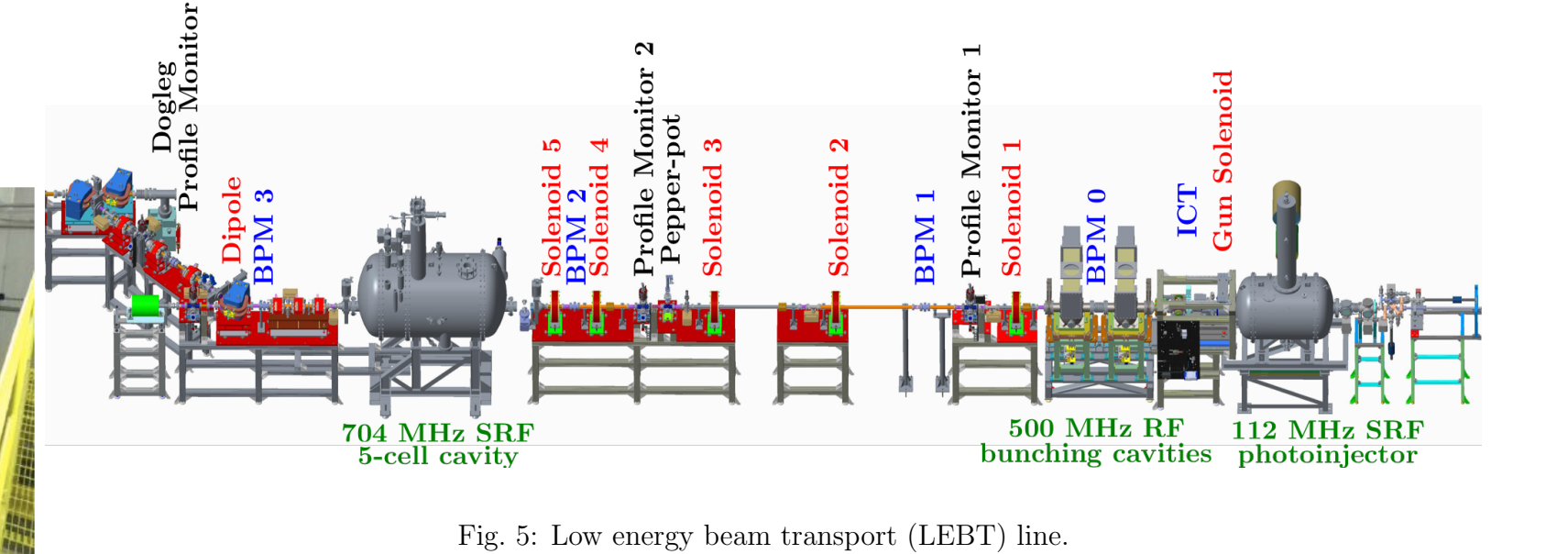


Fig. 5: Low energy beam transport (LEBT) line.

Plasma-Cascade Instability

The PCI is a microwave instability occurring in beams which propagate in a straight line, and is driven by modulation of the electron beam density via transverse focusing. The resulting modulation of the frequency of the plasma oscillations can result in a strong exponentially growing longitudinal instability.

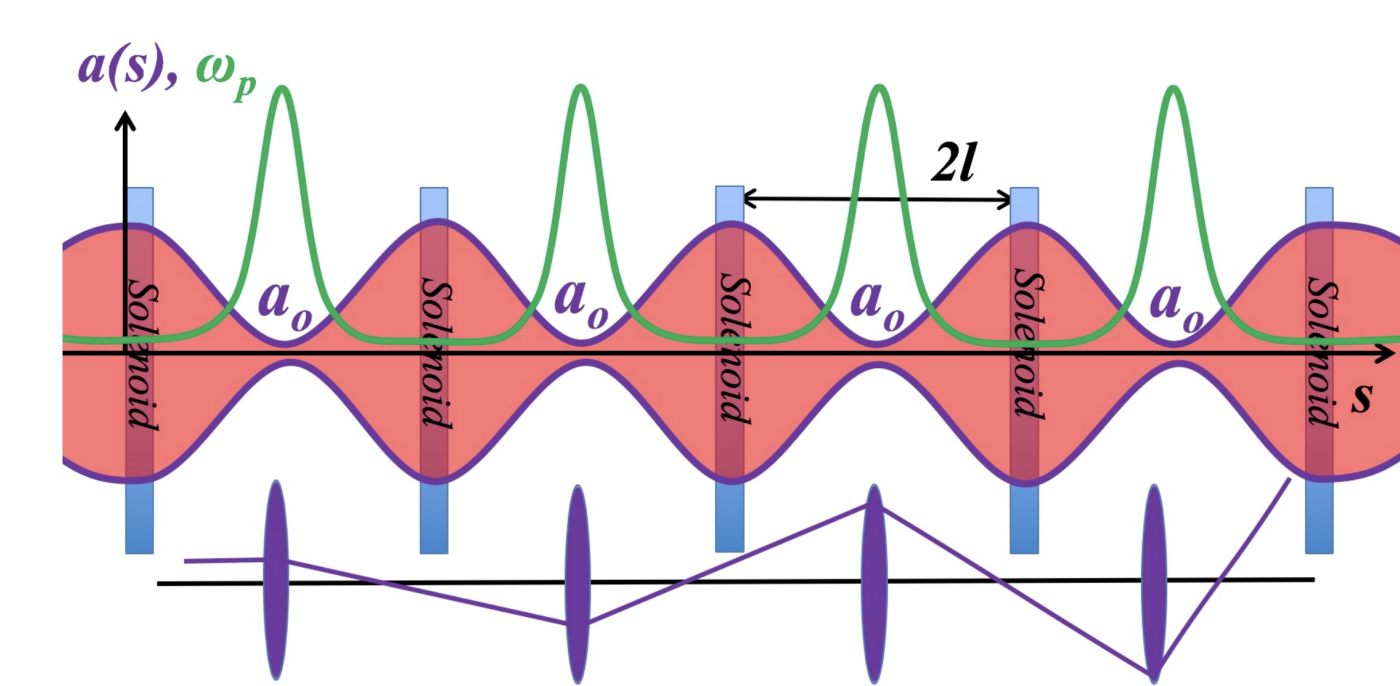


Fig. 6: A sketch of four focusing cells with periodic modulations of beam envelope, $a(s)$ (purple with red shading), and the plasma frequency, ω_p (green outline). Beam envelope has waists, a_0 , in the middle of each cell where plasma frequency peaks. Scales are attuned for illustration purpose. The bottom sketch illustrates an unstable ray trajectory in a system of periodic focusing lenses—an analog of unstable longitudinal oscillations. The waists of the beam serve as “short focusing elements” for the longitudinal plasma oscillations.

Let us consider a cold, homogeneous infinite electron beam of density n . A small perturbation of the beam density, $\delta n \ll n$, will cause oscillations within the beam with plasma frequency $\omega_p = \sqrt{\frac{4\pi n e^2}{m}}$, which can be described by the equation of plasma oscillations:

$$\frac{d^2 \tilde{n}}{dt^2} + \omega_p^2 \tilde{n} = 0, \text{ with } \tilde{n} = n + \delta n \quad (1)$$

Assume that the beam is propagating through a periodic focusing lattice consisting of 5 solenoids, or 4 focusing cells (see Fig. 6). The system provides a periodic transverse beam size modulation, which causes a periodic modulation of the beam density. This density modulation will be inversely proportional to the square of the beam radius a , which would lead to a corresponding modulation of the plasma frequency. Modulation of the plasma frequency is shown in green, and its maxima fall onto the minima (waist) of the transverse beam envelope. These plasma oscillations will lead to the subsequent modulation of the longitudinal density of the beam.

When the oscillator frequency is modulated with a period close to a half of oscillation period, it results in an exponential growth of oscillation amplitude: the phenomenon known as parametric resonance, which leads to an instability. The set of two coupled second order differential equations (see Eq. 2) gives a complete description of the PCI: the transverse envelope equation and the equation for the longitudinal density modulation \tilde{q}_k .

$$\begin{cases} \frac{d^2 \tilde{a}}{ds^2} - \frac{k_{sc}^2}{a} - \frac{k_{\beta}^2}{a^3} = 0, \\ \frac{d^2 \tilde{q}_k}{ds^2} + \frac{2k_{sc}^2}{a^2} - \tilde{q}_k = 0 \end{cases} \quad (2)$$

Here we utilize a set of dimensionless parameters inherited from [3], with normalized beam envelope $\tilde{a} = \frac{a}{a_0}$, where a_0 is the beam waist; $\tilde{s} = \frac{s}{l}$ is the longitudinal distance s normalized to the half of the lattice period. The beam envelope inside the cell is fully determined by the two dimensionless parameters: the space charge, $k_{sc} = \sqrt{\frac{2}{\beta^3 \gamma^3} \frac{I_0 l^2}{I_a a_0^2}}$, and the geometric (or emittance), $k_{\beta} = \frac{e l}{a_0^2}$. Here we denote the beam current as I_0 , and $I = \frac{mc^3}{e}$ is the Alfvén current.

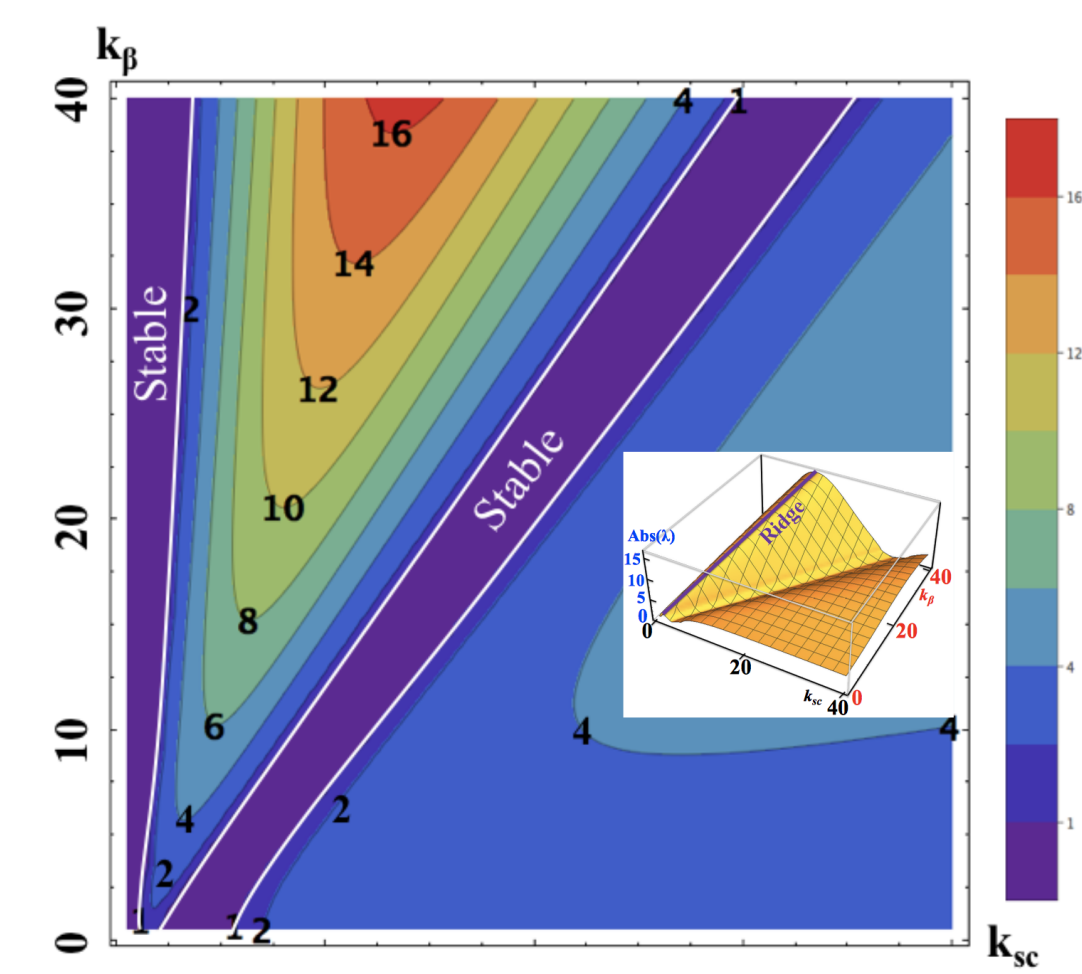


Fig. 7: Contour plots of the absolute value of the growth rate per cell. Purple area highlighted by white lines indicates the areas of the stable oscillations. Density modulation grows exponentially outside these areas. The 3D form of this graph in the inset shows clearly identifiable ridge along the $k_{\beta} = 3(k_{sc} - 1.2)$ line, where the growth rates peak.

Figure 7 demonstrates the growth rate in one cell of the system which depends on the above mentioned parameters. The plot defines the stable and unstable regions of the solution, indicating that the growth rate peaks along the ridge $k_{\beta} = 3(k_{sc} - 1.2)$.

Suppression of the PCI

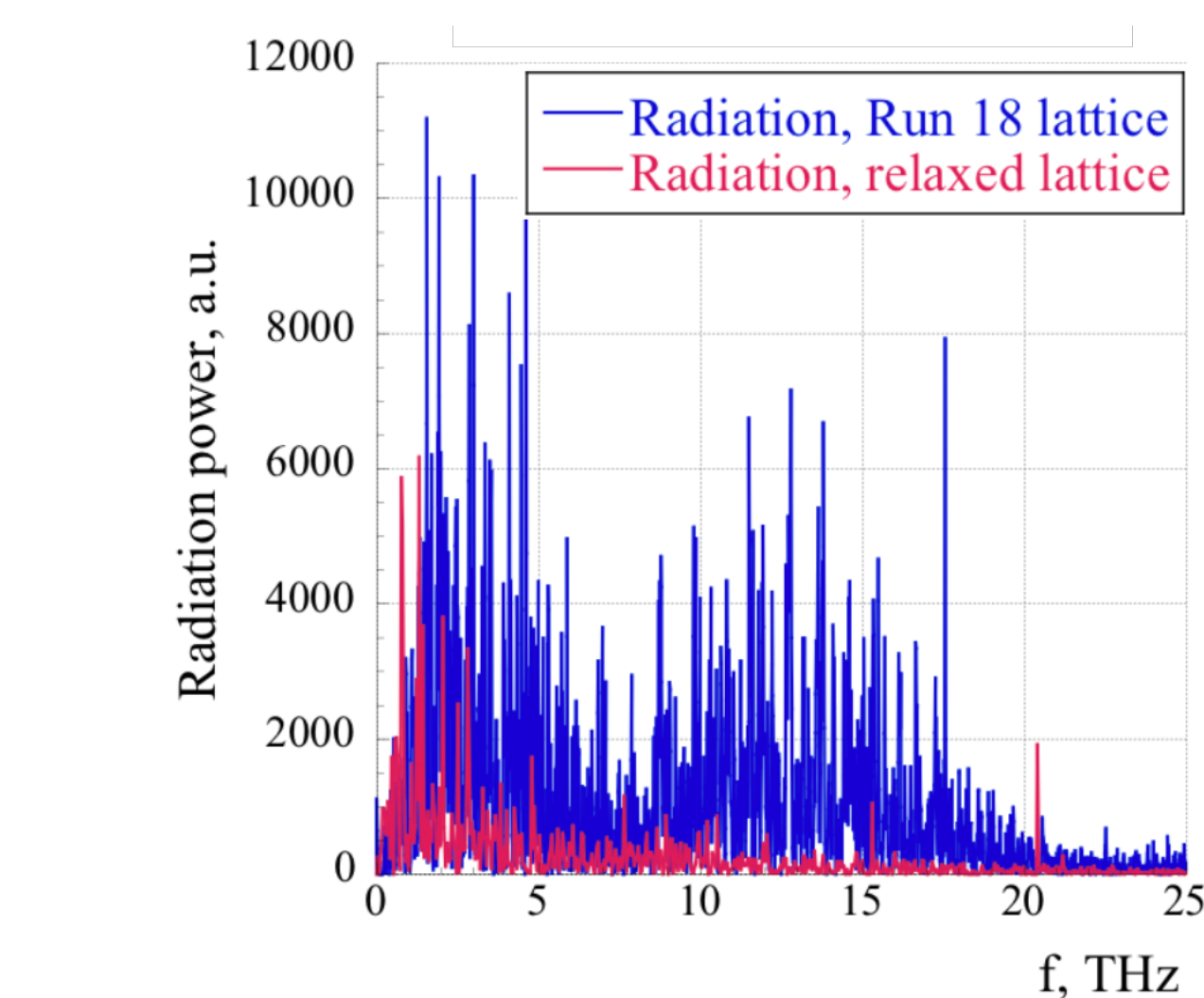


Fig. 8: Radiation spectrum of the compressed 0.7 nC electron bunch at the exit of the SRF linac simulated by IMPACT-T for standard CeC lattice (blue) and relaxed lattice (red).

Figure 8 shows the comparison between the radiation power spectra obtained for the lattice used during the CeC PoP demonstration experiment and a so-called relaxed lattice specifically designed for noise suppression. The result clearly demonstrates that the PCI can be suppressed at the frequencies around 10 THz, when compared to the radiation power spectra for the regular lattice.

We dedicated our experiment in 2019 to the extensive study of the PCI suppression with the goal to demonstrate the ability to deliver a quiet beam with the noise level applicable for the future cooling experiments. The IR detector was installed at the end of the beamline for the characterization of the synchrotron radiation in the THz range from the bending magnet due to the longitudinal density modulation in the beam.

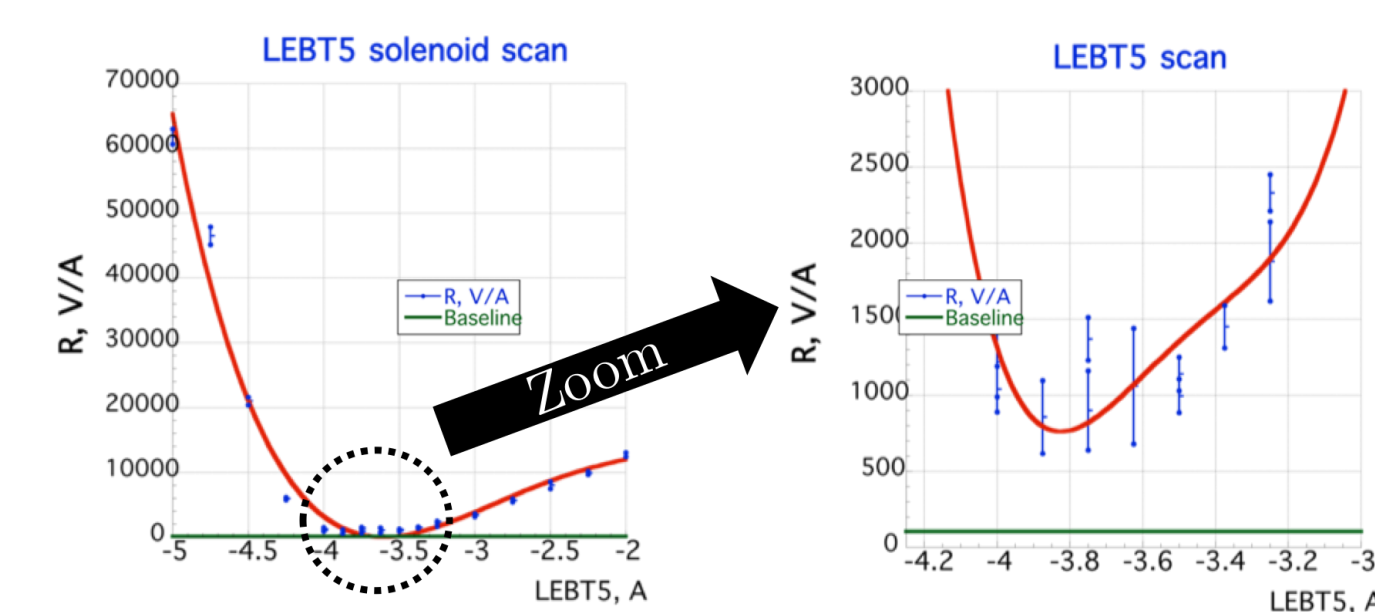


Fig. 9: IR signal as a function of current in LEBT 5 solenoid.

The baseline of the radiation was established for a slightly (4-fold) compressed beam in a relaxed LEBT lattice. Averaged over 4 long scans, the lock-in amplifier signal for the baseline was found to be about 145 V/C. The minimal goal for the experiment was to demonstrate that the ratio of the noise from the PCI to the shot noise in the electron beam can be reduced to 100 and below. As a result of the lattice optimization we were able to achieve a noise level exceeding the shot noise by only a factor of 4 to 10 for a large range of the lattices.

Applications of the PCI—Plasma-Cascade Amplifier

The newly discovered instability has become the base of a new scheme for the CeC amplifier. The new amplifier scheme is broadband, rather simple, cost effective, and doesn't require separation of the ion and electron beams compared to the other schemes alternative to the FEL. A simple schematic of a PCI amplifier (PCA) is shown in Fig. 10. Figure 11 demonstrates the proposed layout for the future PCA-based CeC PoP experiment.

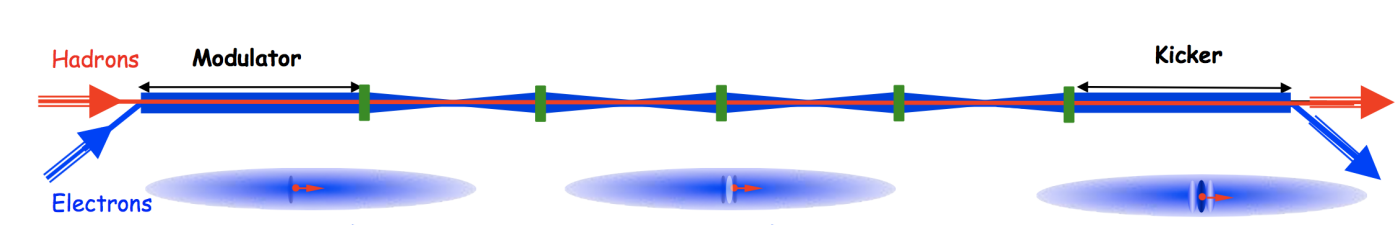


Fig. 10: Schematics of CeC with a Plasma-Cascade Amplifier.

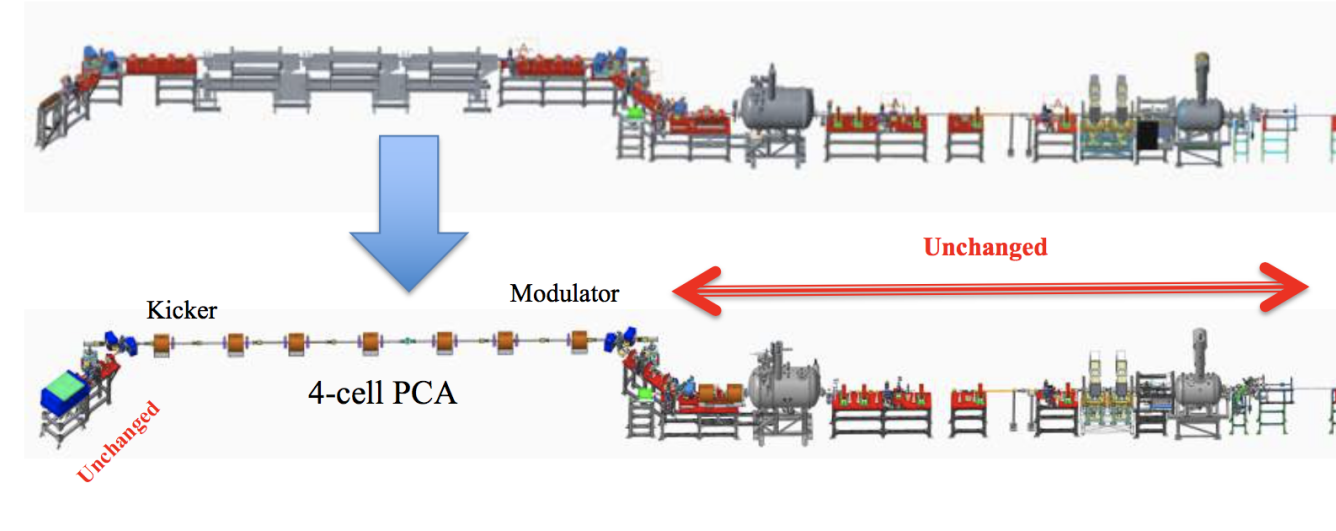


Fig. 11: Schematics of the transition between the FEL-based CeC and the PCA-based CeC.

CeC PoP Demonstration Experiment—Unexpected Results

The essential indicator of the ion and electron beam interactions in the modulator section is a significant increase in the FEL power. When co-propagating through the modulator, each ion creates a corresponding density modulation within the electron beam. The density modulation in this case is defined by the Debye screening and results in a formation of electron beam clouds around every ion.

The figure of merit in the ion imprint study was the relative increase of the FEL intensity, R :

$$R = \frac{I_{\text{overlap}} - I_{\text{separated}}}{I_{\text{separated}}} \quad (3)$$

where I_{overlap} is the intensity of the FEL signal measured with the overlapped beams, and $I_{\text{separated}}$ is the FEL signal measured when the beams were separated longitudinally. The measurements were performed in a wide range of the beam energy ($\pm 5\%$) to demonstrate that the maximum FEL power will be achieved when the beams are overlapped transversely, longitudinally and are moving with the same speed. However, none of the measurements showed the expected increase in the FEL power.

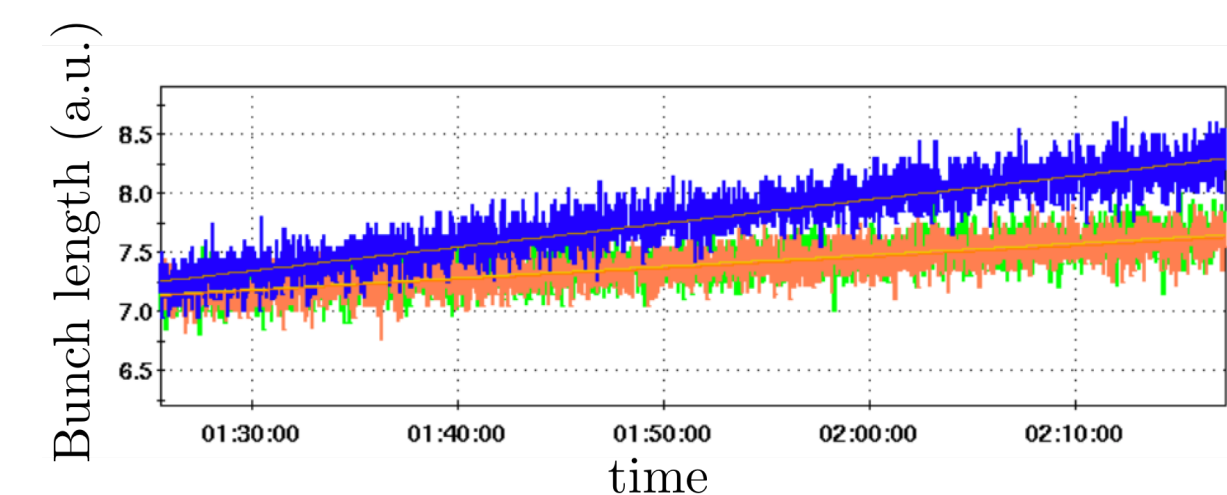


Fig. 12: Evolution of the ion bunch length for interacting (blue) and witness (orange and green) ion bunches.

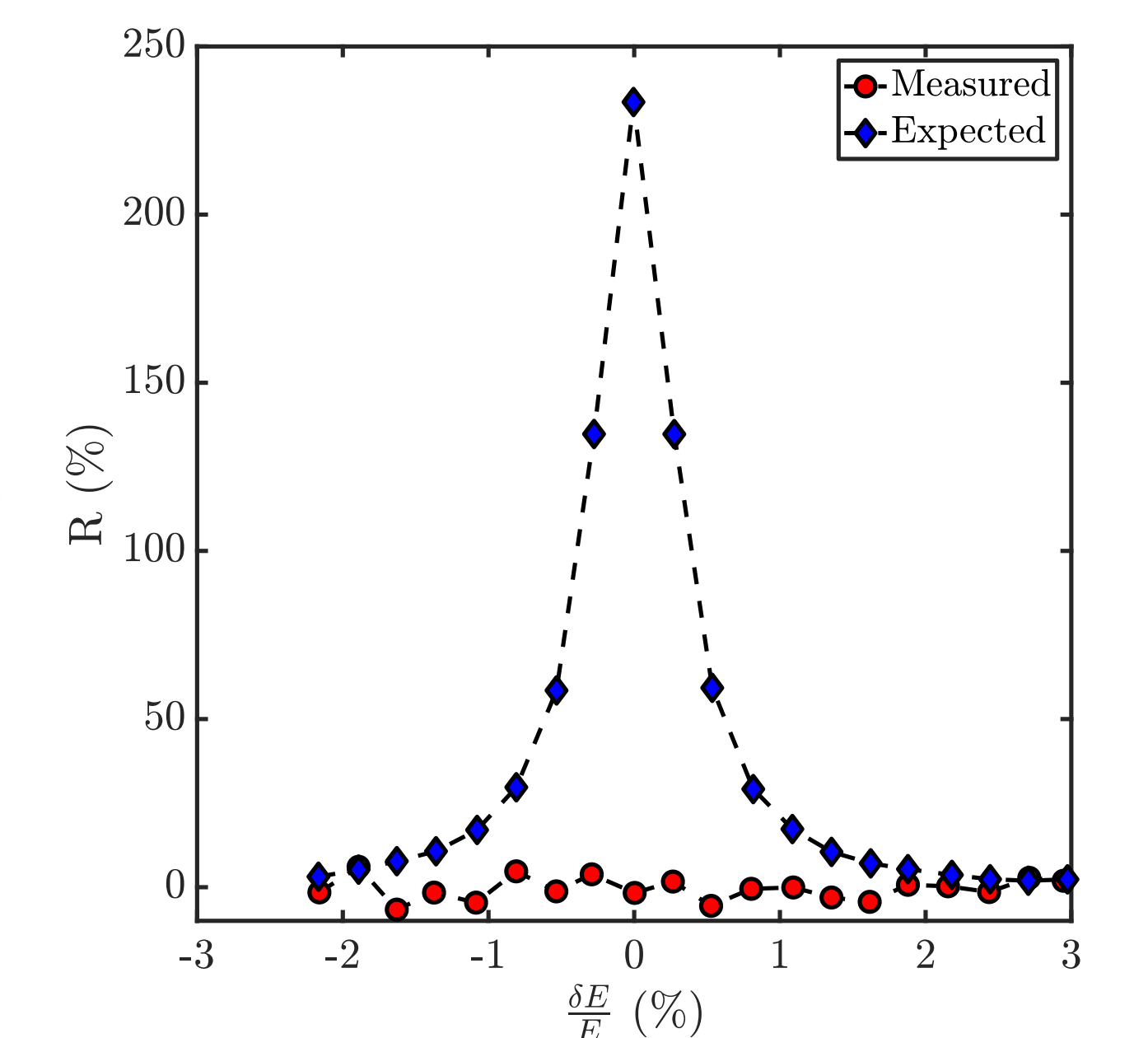


Fig. 13: Relative increase of the FEL intensity as a function of the relative deviation of the beam's relativistic factor.

With the 6 ion bunches circulating in RHIC, we established CW FEL operation with a high-charge (1.2-1.5 nC) electron beam, and overlapped one of the ion beams with the CeC beam. The bunch length of the ion beam under test increased, which indicates that there is, indeed, an interaction between the ion and electron bunches. When the FEL lasing was turned off (to eliminate lasing in the FEL, we reduced the peak current of the electron beam by detuning the buncher cavities), the heating of the ion beam stopped.

Experimental Observations of the PCI

To detect the presence of a density modulation within the beam, we attempted to study the longitudinal beam profile by utilizing the combination of the 45° dipole and the off-resonant operation of the 5-cell 704 MHz SRF cavity. Due to the lack of a dedicated beamline for diagnostics, we established operation of the 5-cell cavity at zero crossing with low accelerating voltage of $V \sim 100-200$ kV, which allowed us to correlate particle's energy with the arrival time. The dipole and the profile monitor located in the dogleg served as the energy spectrometer.

Figure 14 demonstrates a clear dependence of the PCI on the beam charge: the structures vanish below 100 pC, and enhance with increased charge.

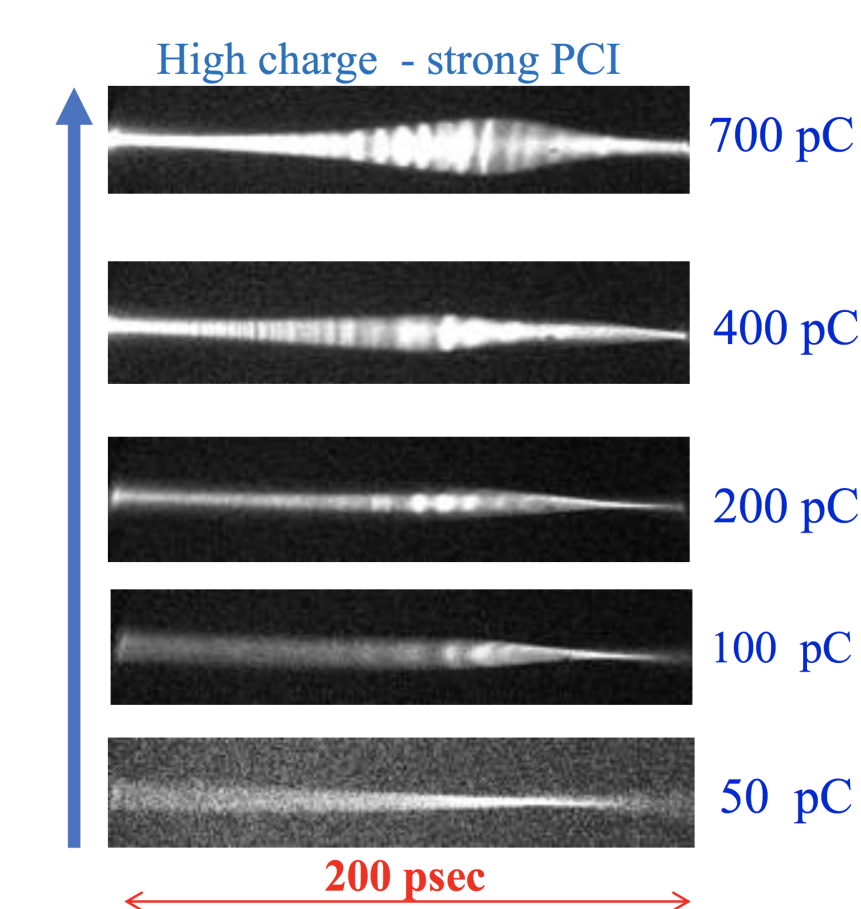


Fig. 14: A set of randomly selected structures measured for uncompressed electron bunches with charge ranging from 50 pC to 700 pC per bunch. Density modulation diminishes at low bunch charges < 100 pC, but becomes very prominent with increasing charge per bunch.

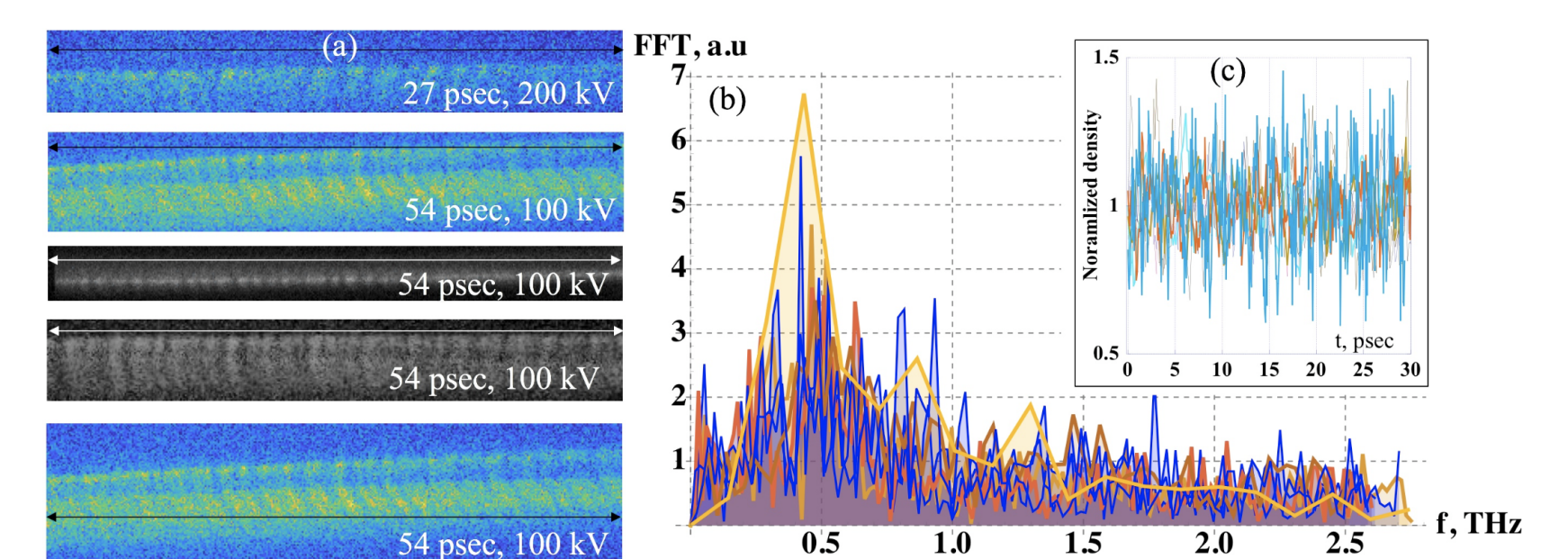


Fig. 15: Analysis of the bunch time profiles for various charges: (a) measured time profiles for charges from 0.45 nC (top) to 0.7 nC (bottom); (b) seven overlapping spectra of measured bunch density modulation and the PCI spectrum simulated by SPACE (slightly elevated yellow line); (c) a 30-psec fragment of seven measured relative density modulations.

The post-processing of several randomly selected time profiles measured for various beam charges from 0.45 to 0.7 nC clearly indicated a strong density modulation along the beam. The FFT of the time profiles showed a good agreement with the result of simulations performed with the code SPACE [6, 7], and demonstrated a prominent peak at 0.4 THz. For the CeC operation we were compressing 400 psec electron bunches with a charge of 0.7-1.4 nC to a peak current of 50-100 A. This required ~ 20 -fold compression of the electron beam, which proportionally shifted the frequency of the density modulation to around 10 THz.

Acknowledgments

This research used resources of the National Energy Research Scientific Computing Center, which is supported by the Office of Science of the U.S. Department of Energy under Contract No. DE-AC02-05CH11231. Work is supported by Brookhaven Science Associates, LLC under Contract No. DEAC0298CH10886 with the U.S. Department of Energy, DOE NP office grant DE-FOA-0000632, and NSF grant PHY-1415252.

References

- [1] V.N. Litvinenko and Ya.S. Derbenev, “Coherent electron cooling”, *Phys. Rev. Accel. Beams*, vol. 102, p. 114801, 2009.
- [2] I. Pinayev *et al.*, “Performance of CeC PoP Accelerator”, in *Proc. 10th Int. Particle Accelerator Conf. (IPAC'19)*, Melbourne, Australia, May 2019, pp. 559–561. doi:10.18429/JACoW-IPAC2019-MOPMP050
- [3] V.N. Litvinenko *et al.*, “Plasma-Cascade micro-bunching Amplifier and Coherent electron Cooling of a Hadron Beams”, *arXiv preprint arXiv:1802.08677*, 2018.
- [4] V.N. Litvinenko *et al.*, “Plasma-Cascade Instability—theory, simulations and experiment”, *arXiv preprint arXiv:1902.10846*, 2019.
- [5] I. Petrushina *et al.*, “High Brightness CW Electron Beams From Superconducting RF Photoinjector”, presented at the North American Particle Accelerator Conference (NAPAC'19), Lansing, Michigan, September 2019, MOZBB4, this conference.
- [6] X. Wang *et al.*, “AP-Cloud: Adaptive Particle-in-Cloud method for optimal solutions to Vlasov–Poisson equation”, *Journal of Computational Physics*, vol. 316, pp. 682–699, 2019.
- [7] K. Yu and V. Samulyak, “SPACE Code for Beam-Plasma Interaction”, in *Proc. 6th Int. Particle Accelerator Conf. (IPAC'15)*, Richmond, VA, USA, May 2015, pp. 728–730. doi:10.18429/JACoW-IPAC2015-MOPMN012
- [8] “IMPACT-T: A 3D Parallel Particle Tracking Code in Time Domain”, <https://amac.lbl.gov/jiqiang/IMPACT-T/index.html>.